

## **Recent Developments in Material Microstructure: a Theory of Coarsening**

K. Barmak, E. Eggeling, M. Emelianenko, Y. Epshteyn, D. Kinderlehrer, R. Sharp, and S. Ta'asan

### **ABSTRACT**

Cellular networks are ubiquitous in nature. Most engineered materials are polycrystalline microstructures composed of a myriad of small grains separated by grain boundaries, thus comprising cellular networks. The recently discovered grain boundary character distribution (GBCD) is an empirical distribution of the relative length (in 2D) or area (in 3D) of interface with a given lattice misorientation and normal. During the coarsening, or growth, process, an initially random grain boundary arrangement reaches a steady state that is strongly correlated to the interfacial energy density. In simulation, if the given energy density depends only on lattice misorientation, then the steady state GBCD and the energy are related by a Boltzmann distribution. This is among the simplest non-random distributions, corresponding to independent trials with respect to the energy. Why does such simplicity emerge from such complexity? Here we describe an entropy based theory which suggests that the evolution of the GBCD satisfies a Fokker-Planck Equation, an equation whose stationary state is a Boltzmann distribution.

### **1. INTRODUCTION**

Cellular networks are ubiquitous in nature. They exhibit behavior on many different length and time scales and are generally metastable. Most technologically useful materials are polycrystalline microstructures composed of a myriad of small monocrystalline grains separated by grain boundaries, and thus comprise cellular networks. The energetics and connectivity of the grain boundary network plays a crucial role in determining the properties of a material across a wide range of scales. A central problem is to develop technologies capable of producing an arrangement of grains that provides for a desired set of material properties. Traditionally our focus has been on distributions of geometric features, like cell size, and a preferred distribution of grain orientations, termed texture. Attaining these gives the configuration order in a statistical sense.

During coarsening, it is the cell boundaries that are changing, so any order in the configuration is conferred by this boundary network. Recent mesoscale experiment and simulation permit harvesting large amounts of information about both geometric features and crystallography of the boundary network in material microstructures, [1],[2],[23],[29],[30]. This has led us to the introduction of the Grain Boundary Character Distribution (GBCD). The grain boundary character distribution is an empirical distribution of the relative length (in 2D) or area (in 3D) of interface with a given lattice misorientation and grain boundary normal. We now describe two discoveries. The first is that during the growth process, an initially random grain boundary arrangement reaches a steady state that is strongly correlated to the interfacial energy density. In simulation, a stationary GBCD is always found. Moreover there is consistency between experimental GBCD's and simulated GBCD's, [23]. The boundary network of a cellular structure is naturally ordered.

A second discovery is that if the given interfacial energy depends only on lattice misorientation, then the steady state GBCD and the energy density are related by a Boltzmann distribution. This is among the simplest non-random distributions, corresponding to independent trials with respect to the density. Such straightforward dependence between the character distribution and the interfacial energy offers evidence that the GBCD is a material property. Thus there is a natural order to the

grain boundary network. The GBCD becomes a leading candidate to characterize texture of the boundary network [23].

Here we summarize our recent work developing an entropy based theory that suggests that the evolving GBCD satisfies a Fokker-Planck Equation, [5],[11], cf. also [6], [4],[12] to which we refer for a more complete exposition. Coarsening in polycrystalline systems is a complicated process involving details of material structure, chemistry, arrangement of grains in the configuration, and environment. In this context, we consider just two competing global features, as articulated by C. S. Smith [31]: cell growth according to a local evolution law and space filling constraints. We shall impose curvature driven growth for the local evolution law, cf. Mullins [28]. Space filling requirements are managed by critical events, rearrangements of the network involving deletion of small contracting cells and facets. The behavior of the system is then embodied in a dissipation relation. With this relation, the properties of this system that characterize the GBCD must be identified and appropriately upscaled or ‘coarse-grained’. Indeed, we have no direct way to determine the stationary GBCD. In fact, we direct our attention to a deeper result. The kinetics of the GBCD, its trajectory as a function of time, are identified as resembling the mass transport implicit scheme for the Fokker-Planck equation [20]. This will be described further ahead in the text. For a perspective on these issues, we recommend the article by R. V. Kohn [26]. To our knowledge, this, and the simplified model of Section 3, are the first experimental systems whose kinetics are identified by the mass transport implicit scheme of [20].

The general platform for this investigation is large scale computation. The laboratory is the venue to assess the validity of the local evolution law. Once this law is adopted, we appeal to simulation, since we cannot control all the elements present in the experimental system, many of which are unknown. On the other hand, *in silico* we may exercise, or at least we may attempt to exercise, precise control of the variables appropriate to the evolution law and the constraint.

## 2. MESOSCALE THEORY

The common denominator theory for the mesoscale description of microstructure evolution is curvature driven growth, the Mullins Equation (2.2) below, for the evolution of curves or arcs individually or in a network. We employ this for our local law of evolution. Boundary conditions must be imposed where the arcs meet. This condition is the Herring Condition, (2.3), which is the natural boundary condition at equilibrium for the Mullins Equation. Since their introduction by Mullins, [28], and Herring, [18], [19], a large and distinguished body of work has grown about these equations. Most relevant to here are [17], [14], [22]. Curvature driven growth has classical origins, dating at least to Burke and Turnbull [15]. Let  $\alpha$  denote the misorientation between two grains separated by an arc  $\Gamma$ , as noted in Figure 1, with normal  $n = (\cos \theta, \sin \theta)$ , tangent direction  $b$  and curvature  $\kappa$ . Let  $\psi = \psi(\theta, \alpha)$  denote the energy density on  $\Gamma$ . So

$$\Gamma : x = \xi(s, t), \quad 0 \leq s \leq L, \quad t > 0, \quad (2.1)$$

with

$$b = \frac{\partial \xi}{\partial s} \text{ (tangent) and } n = Rb \text{ (normal)}$$

$$v = \frac{\partial \xi}{\partial t} \text{ (velocity) and } v_n = v \cdot n \text{ (normal velocity)}$$

where  $R$  is a positive rotation of  $\pi/2$ . The Mullins Equation of evolution is

$$v_n = (\psi_{\theta\theta} + \psi)\kappa \text{ on } \Gamma. \quad (2.2)$$

We assume that only triple junctions are stable and that the Herring Condition holds at triple junctions. This means that whenever three curves,  $\{\Gamma^{(1)}, \Gamma^{(2)}, \Gamma^{(3)}\}$ , meet at a point  $p$  the force

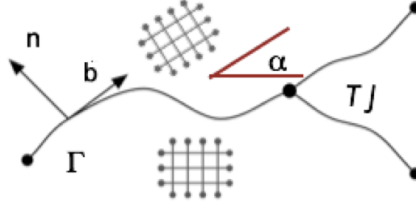


FIGURE 1. An arc  $\Gamma$  with normal  $n$ , tangent  $b$ , and lattice misorientation  $\alpha$ , illustrating lattice elements.

balance, (2.3) below, holds:

$$\sum_{i=1,\dots,3} (\psi_\theta n^{(i)} + \psi b^{(i)}) = 0. \quad (2.3)$$

Consider a network of grains bounded by  $\{\Gamma_i\}$  subject to some condition at the border of the region they occupy, like fixed end points or periodicity. For the description of the algorithms used in the simulation, the reader can consult [24],[21]. The typical simulation consists in initializing a configuration of cells and their boundary arcs, usually by a modified Voronoi tessellation, and then solving the system (2.2), (2.3), eliminating facets when they have negligible length and cells when they have negligible area. The total energy of the system is given by

$$E(t) = \sum_{\{\Gamma_i\}} \int_{\Gamma_i} \psi |b| ds. \quad (2.4)$$

Owing to the Herring Condition (2.3), in an interval  $(t_0, t_0 + \tau)$  where there are no critical events, we obtain the dissipation relation

$$\sum_{\{\Gamma_i\}} \int_{t_0}^{t_0+\tau} \int_{\Gamma_i} v_n^2 ds dt + E(t_0 + \tau) = E(t_0) \quad (2.5)$$

which bears a strong resemblance to the simple dissipation relation for an ensemble of inertia free springs with friction. In the simulation, the facet interchange and cell deletion are arranged so that (2.5) is maintained as an inequality.

Suppose, for simplicity, that the energy density is independent of the normal direction, so  $\psi = \psi(\alpha)$ , the situation that will concern us here. Then (2.2) and (2.3) may be expressed

$$v_n = \psi \kappa \text{ on } \Gamma \quad (2.6)$$

$$\sum_{i=1,\dots,3} \psi b^{(i)} = 0 \text{ at } p, \quad (2.7)$$

where  $p$  denotes a triple junction. (2.7) is the same as the Young wetting law.

For this situation we define the grain boundary character distribution, GBCD,

$$\begin{aligned} \rho(\alpha, t) &= \text{relative length of arc of misorientation } \alpha \text{ at time } t, \\ &\text{normalized so that } \int_{\Omega} \rho d\alpha = 1. \end{aligned} \quad (2.8)$$

### 3. A SIMPLIFIED COARSENING MODEL WITH ENTROPY AND DISSIPATION

A significant difficulty in developing a theory for the GBCD, and understanding texture development in general, lies in the lack of understanding of consequences of rearrangement events or critical events, facet interchange and grain deletion, on network level properties. For example, in Fig. 2, the average area of five-faceted grains during a growth experiment on an  $Al$  thin film and

the average area of five-faceted cells in a typical simulation both increase with time. Now the von Neumann-Mullins Rule is that the area  $A_n$  of a cell with  $n$ -facets satisfies

$$A'_n(t) = c(n - 6), \quad (3.1)$$

when  $\psi = \text{const.}$  and triple junctions meet at angles of  $2\pi/3$ , [27], [32]. This is thought to hold approximately when anisotropy is small. The von Neumann-Mullins Rule does not fail in the example above, of course, but cells observed at later times had 6, 7, 8, ... facets at earlier times. Thus in the network setting, changes which rearrange the network play a major role.

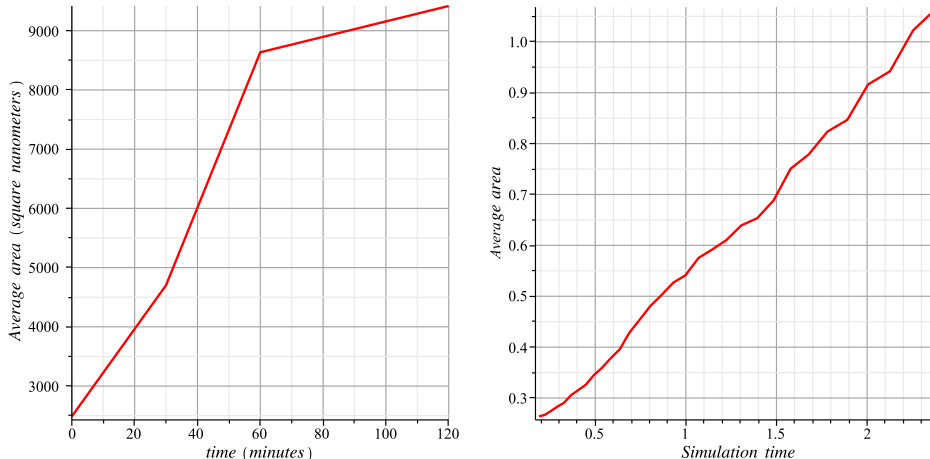


FIGURE 2. The average area of five-sided cell populations during coarsening in two different cellular systems showing that the von Neumann-Mullins  $n - 6$ -Rule (3.1) does not hold at the scale of the network. (left) In an experiment on *Al* thin film, [7], and (right) a typical simulation (arbitrary units).

To address these issues, we will examine a much simpler 1 D model which retains kinetics and critical events but neglects curvature driven motion of the boundaries. We have used this model to develop a statistical theory for critical events, [9], [10], [8]. It has been found to have its own GBCD as well, [4], [6], [5], [11], which we shall now review.

Our main idea in [4], [6], [5], [11] is that the GBCD statistic for the simplified model resembles the solution of a Fokker-Planck Equation via the mass transport implicit scheme, [20]. In [4], [6], [5], [11] the simplified model is formulated as a gradient flow which results in a dissipation inequality analogous to the one found for the coarsening grain network. Because of this simplicity, it will be possible to ‘upscale’ the network level system description to a higher level GBCD description that accommodates irreversibility. A more useful dissipation inequality is obtained by modifying the viscous term to be a mass transport term, which now brings us to the realm of the Kantorovich-Rubinstein-Wasserstein implicit scheme. As this changes the ensemble, there is an entropic contribution, which we take to be proportional to configurational entropy. This then suggests the Fokker-Planck paradigm which we describe in Section 3.2.

We do not know, of course, that the statistic is a solution of the Fokker-Planck PDE but we can ask if it shares important aspects of Fokker-Planck behavior. We give evidence for this by asking for the unique ‘temperature-like’ parameter, the factor noted above, the relative entropy achieves a minimum over long time. The empirical stationary distribution and Boltzmann distribution with the special value of ‘temperature’ are in excellent agreement. This gives an explanation for the stationary distribution and the kinetics of evolution. Although we are not presenting arguments that two dimensional network has the detailed dissipative structure of the simplified model, we are able to produce evidence that the same argument employing the relative entropy does suggest the correct kinetics and stationary distribution.

**3.1. Formulation.** The simplified coarsening model, driven by the boundary conditions, reflects the dissipation relation of the grain growth system. It also resembles an ensemble of inertia-free spring-mass-dashpots. It is an abstraction of the role of triple junctions in the presence of the rearrangement events. We give a careful formulation. Let  $I \subset \mathbf{R}$  be an interval of length  $L$  partitioned by points  $x_i, i = 1, \dots, n$ , where  $x_i < x_{i+1}, i = 1, \dots, n-1$  and  $x_{n+1}$  identified with  $x_1$ . For each interval  $[x_i, x_{i+1}], i = 1, \dots, n$  select a random misorientation number  $\alpha_i \in (-\pi/4, \pi/4]$ . The intervals  $[x_i, x_{i+1}]$  correspond to grain boundaries (but not the 1D “grain”) with misorientations  $\alpha_i$  and the points  $x_i$  represent the triple junctions. Choose an energy density  $\psi(\alpha) \geq 0$  and introduce the energy

$$E = \sum_{i=1, \dots, n} \psi(\alpha_i)(x_{i+1} - x_i). \quad (3.2)$$

To have consistency with the evolution of the 2D cellular network, we impose gradient flow kinetics with respect to (3.2), which is just the system of ordinary differential equations

$$\begin{aligned} \frac{dx_i}{dt} &= -\frac{\partial E}{\partial x_i}, i = 1, \dots, n, \text{ that is} \\ \frac{dx_i}{dt} &= \psi(\alpha_i) - \psi(\alpha_{i-1}), i = 2 \dots n, \text{ and } \frac{dx_1}{dt} = \psi(\alpha_1) - \psi(\alpha_n). \end{aligned} \quad (3.3)$$

The velocity  $v_i$  of the  $i^{\text{th}}$  boundary is

$$v_i = \frac{dx_{i+1}}{dt} - \frac{dx_i}{dt} = \psi(\alpha_{i-1}) - 2\psi(\alpha_i) + \psi(\alpha_{i+1}). \quad (3.4)$$

Next consider for the 1D system (3.3), a time interval  $(t_0, t_0 + \tau)$  with no critical events for now. Then we obtain, after some algebra, an analog of the grain growth spring-mass-dashpot-like local dissipation inequality.

$$\frac{1}{4} \sum_{i=1 \dots n} \int_0^\tau v_i^2 dt + E(t_0 + \tau) \leq E(t_0) \quad (3.5)$$

As explained in [6],[5],[11], we can introduce now the idea of GBCD for the simplified 1D model. Let us consider a new ensemble based on the misorientation parameter  $\alpha$  where we take  $\Omega : -\frac{\pi}{4} \leq \alpha \leq \frac{\pi}{4}$ , for later ease of comparison with the two dimensional network for which we are imposing “cubic” symmetry, i.e., “square” symmetry in the plane. The GBCD or character distribution in this context is, as expected, the histogram of lengths of intervals sorted by misorientation  $\alpha$  scaled to be a probability distribution on  $\Omega$  as described in (2.8). One may express (3.5) in terms of the character distribution (2.8), which amounts to

$$\mu_0 \int_{t_0}^{t_0+\tau} \int_{\Omega} \left| \frac{\partial \rho}{\partial t}(\alpha, t) \right|^2 d\alpha dt + \int_{\Omega} \psi(\alpha) \rho(\alpha, t_0 + \tau) d\alpha \leq \int_{\Omega} \psi(\alpha) \rho(\alpha, t_0) d\alpha, \quad (3.6)$$

where  $\mu_0 > 0$  is some constant.

The expression (3.6) is in terms of the new misorientation level ensemble, upscaled from the local level of the original system. We now introduce, as discussed earlier, the modeling assumption, consistent with the lack of reversibility when rearrangement/or critical events occur and add an entropic contribution to (3.6). We consider standard configurational entropy,

$$+ \int_{\Omega} \rho \log \rho d\alpha, \quad (3.7)$$

although this is not the only choice. Minimizing (3.7) favors the uniform state, which would be the situation were  $\psi(\alpha) = \text{constant}$ . A tantalizing clue to the development of texture will be whether or not this entropy strays from its minimum during the simulation.

Given that (3.6) holds, we assume now that there is some  $\lambda > 0$  such that for any  $t_0$  and  $\tau$  sufficiently small that

$$\mu_0 \int_{t_0}^{t_0+\tau} \int_{\Omega} \left(\frac{\partial \rho}{\partial t}\right)^2 d\alpha dt + \int_{\Omega} (\psi \rho + \lambda \rho \log \rho) d\alpha|_{t_0+\tau} \leq \int_{\Omega} (\psi \rho + \lambda \rho \log \rho) d\alpha|_{t_0} \quad (3.8)$$

$E(t)$  was analogous to an internal energy or the energy of a microcanonical ensemble and now

$$F(\rho) = F_{\lambda}(\rho) = E(t) + \lambda \int_{\Omega} \rho \log \rho d\alpha \quad (3.9)$$

is a free energy. The value of the parameter  $\lambda$  is unknown and will be determined in the Validation Section 4. Finally, the first term in (3.8) can be estimated from below to represent energy lost due to frictional or viscous forces (for details cf. [11]). This results in the inequality, valid the pair  $v, \rho$

$$\begin{aligned} \frac{\mu}{2} \int_0^{\tau} \int_{\Omega} v^2 \rho d\alpha dt + F_{\lambda}(\rho) &\leq F_{\lambda}(\rho^*) \text{ where} \\ \rho_t + (v\rho)_{\alpha} &= 0, \text{ (continuity equation)} \\ \rho &= \rho|_{t_0+\tau} \text{ and } \rho^* = \rho|_{t_0} \text{ for some fixed } \mu > 0. \end{aligned} \quad (3.10)$$

**3.2. The mass transport paradigm.** Among the equivalent formulations of the Kantorovich-Rubinstein-Wasserstein metric, or simply the Wasserstein metric, by a result of Benamou and Brenier [13], is a minimum principle related to (3.10). Given two probability densities  $\rho^*, \rho$  on  $\Omega$ , this metric  $d$  is

$$\begin{aligned} \frac{1}{\tau} d(\rho, \rho^*)^2 &= \inf \int_0^{\tau} \int_{\Omega} v^2 \rho d\xi dt \\ &\text{over deformation paths } \rho(\xi, t) \text{ subject to} \\ \rho_t + (v\rho)_{\xi} &= 0, \text{ (continuity equation) and} \\ \rho(\xi, 0) &= \rho^*(\xi), \rho(\xi, \tau) = \rho(\xi) \text{ (initial and terminal conditions)} \end{aligned} \quad (3.11)$$

With this in mind, we replace (3.10) by an implicit scheme: Given  $\rho^*$  determine  $\rho$  the solution of the variational problem

$$\frac{\mu}{2\tau} d(\rho, \rho^*)^2 + F_{\lambda}(\rho) = \inf_{\{\eta\}} \left\{ \frac{\mu}{2\tau} d(\eta, \rho^*)^2 + F_{\lambda}(\eta) \right\} \quad (3.12)$$

Now for each relaxation time  $\tau > 0$  we determine iteratively the sequence  $\{\rho^{(k)}\}$  by choosing  $\rho^* = \rho^{(k-1)}$  and  $\rho^{(k)} = \rho$  in (3.12) and setting

$$\rho^{(\tau)}(\alpha, t) = \rho^{(k)}(\alpha) \text{ in } \Omega \text{ for } k\tau \leq t < (k+1)\tau. \quad (3.13)$$

We then anticipate recovering the GBCD  $\rho$  as

$$\rho(\alpha, t) = \lim_{\tau \rightarrow 0} \rho^{(\tau)}(\alpha, t), \quad (3.14)$$

with the limit taken in a suitable sense. It is known that  $\rho$  obtained from (3.14) is the solution of the Fokker-Planck Equation, [20],

$$\mu \frac{\partial \rho}{\partial t} = \frac{\partial}{\partial \alpha} \left( \lambda \frac{\partial \rho}{\partial \alpha} + \psi' \rho \right) \text{ in } \Omega, 0 < t < \infty. \quad (3.15)$$

We might point out here, as well, that a solution of (3.15) with periodic boundary conditions and nonnegative initial data is positive for  $t > 0$ .

Hence the upscaled dissipation inequality (3.10) leads to the implicit scheme (3.12) and thus to the Fokker-Planck Equation (3.15). A further investigation of the intimate connection between the simplified problem and the Ornstein-Uhlenbeck process is forthcoming [3]. A derivation of (3.15) directly for the two-dimensional coarsening system is forthcoming in [25].

#### 4. VALIDATION OF THE SCHEME

We now begin the validation step of our theory. The procedure which leads to the implicit scheme, based on the dissipation inequality (3.5), holds for the entire system but does not identify individual intermediate ‘spring-mass-dashpots’. The consequence is that we cannot set the temperature-like parameter  $\sigma$ , but in some way must decide if one exists. Introduce the notation for the Boltzmann distribution with parameter  $\lambda$

$$\rho_\lambda(\alpha) = \frac{1}{Z_\lambda} e^{-\frac{1}{\lambda}\psi(\alpha)}, \alpha \in \Omega, \text{ with } Z_\lambda = \int_{\Omega} e^{-\frac{1}{\lambda}\psi(\alpha)} d\alpha. \quad (4.1)$$

With validation we would gain qualitative properties of solutions of (3.15):

- $\rho(\alpha, t) \rightarrow \rho_\sigma(\alpha)$  as  $t \rightarrow \infty$ , and
- this convergence is exponentially fast.

We shall approach this by introducing a simple convex duality problem for the Kullback-Leibler relative entropy. It is a maximum likelihood test. The Kullback-Leibler relative entropy for (3.15) is given by

$$\begin{aligned} \Phi_\lambda(\eta) &= \Phi(\eta \| \rho_\lambda) = \int_{\Omega} \eta \log \frac{\eta}{\rho_\lambda} d\alpha = \int_{\Omega} \{\psi_\lambda \eta + \eta \log \eta\} d\alpha \text{ where} \\ \eta &\geq 0 \text{ in } \Omega, \int_{\Omega} \eta d\alpha = 1 \text{ and } \psi_\lambda = \frac{\psi}{\lambda} + \log Z_\lambda. \end{aligned} \quad (4.2)$$

with  $\rho_\lambda$  from (4.1). By Jensen’s Inequality it is always nonnegative. In terms of the free energy (3.9) and (4.1), (4.2) is given by

$$\Phi_\lambda(\eta) = \frac{1}{\lambda} F_\lambda(\eta) + \log Z_\lambda. \quad (4.3)$$

(Note: In our earlier work [5, 11], we defined relative entropy to be  $\lambda$  times (4.2).) A solution  $\rho$  of (3.15) has the property that

$$\Phi_\lambda(\rho) \rightarrow 0 \text{ as } t \rightarrow \infty. \quad (4.4)$$

Therefore, we seek to identify the particular  $\lambda = \sigma$  for which  $\Phi_\sigma$  defined by the GBCD statistic  $\rho$  tends monotonically to the minimum of all the  $\{\Phi(\rho \| \rho_\lambda)\}$  as  $t$  becomes large. We then ask if the terminal, or equilibrium, empirical distribution  $\rho$  is equal to  $\rho_\sigma$ . Now the manifold of functions  $\{\psi_\lambda\}$  is a strictly convex in terms of the ‘inverse temperature’  $\beta = \frac{1}{\lambda}, \beta > 0$ , and thus there is a unique  $\psi_\sigma$  such that

$$\int_{\Omega} \{\psi_\sigma \rho + \rho \log \rho\} d\alpha = \inf_{\{\psi_\lambda\}} \int_{\Omega} \{\psi_\lambda \rho + \rho \log \rho\} d\alpha. \quad (4.5)$$

The information theory interpretation of (4.5) is that we are minimizing the information loss among trial encodings of the alphabet represented by the statistic  $\rho$ . In this sense we see that asking for an optimal distribution  $\rho_\sigma$  to represent our statistic  $\rho$ , necessarily introduces (relative) entropy in our considerations, returning us, as it were, full circle. This also is similar to a large deviation principle.

#### 5. THE ENTROPY METHOD FOR THE GBCD

We shall apply the method of Section 4 to the GBCD harvested from the 2D simulation. Here we present only a typical simulation with the energy density

$$\psi(\alpha) = 1 + \epsilon(\sin 2\alpha)^2, \quad -\frac{\pi}{4} \leq \alpha \leq \frac{\pi}{4}, \quad \epsilon = 1/2, \quad (5.1)$$

Figure 3, initialized with  $10^4$  cells and normally distributed misorientation angles and terminated when 2000 cells remain. At this stage, the simulation is essentially stagnant. Five trials were executed and we consider the average of  $\rho$  of the empirical GBCD’s. Possible ‘temperature’ parameters

$\lambda$  and  $\rho_\lambda$  in (4.1) for the density (5.1) are constructed. This  $\rho_\lambda$  then defines a trial relative entropy via (4.2). We now identify the parameter  $\sigma$ , which turns out to be  $\sigma \approx 0.1$ , and the value of the relative entropy  $\Phi_\sigma(T_\infty) \approx 0.01$ , which is about 10% of its initial value, Figure 4. From Figure 5 (left), we see that this relative entropy  $\Phi_\sigma$  has exponential decay until it reaches time about  $t = 1.5$ , after which it remains constant. The averaged empirical GBCD is compared with the Boltzmann distribution in Figure 5 (right). The solution itself then tends exponentially in  $L^1$  to its limit  $\rho_\sigma$  by the Kullback-Leibler Inequality.

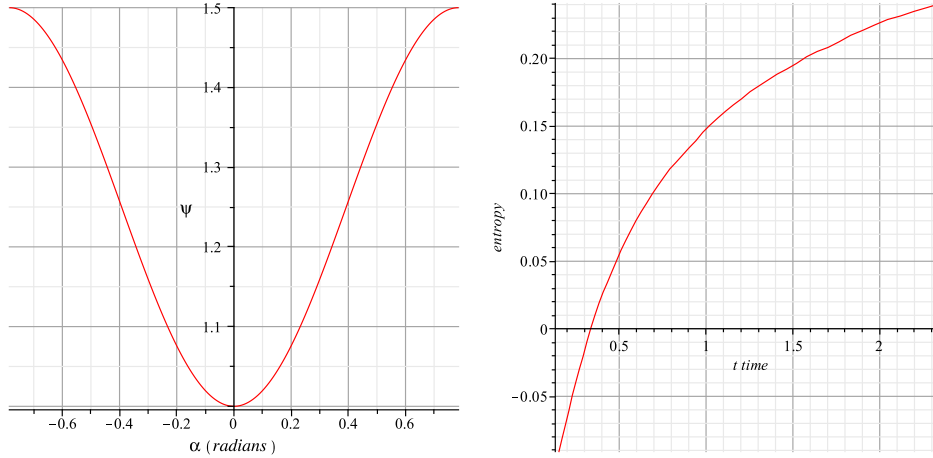


FIGURE 3. (left) The energy density  $\psi(\alpha) = 1 + \epsilon \sin^2 2\alpha$ ,  $|\alpha| < \pi/4$ ,  $\epsilon = \frac{1}{2}$ . (right) The configurational entropy of  $\rho(\alpha, t)$  as a function of time  $t$  is increasing, suggesting the development of order in the configuration.

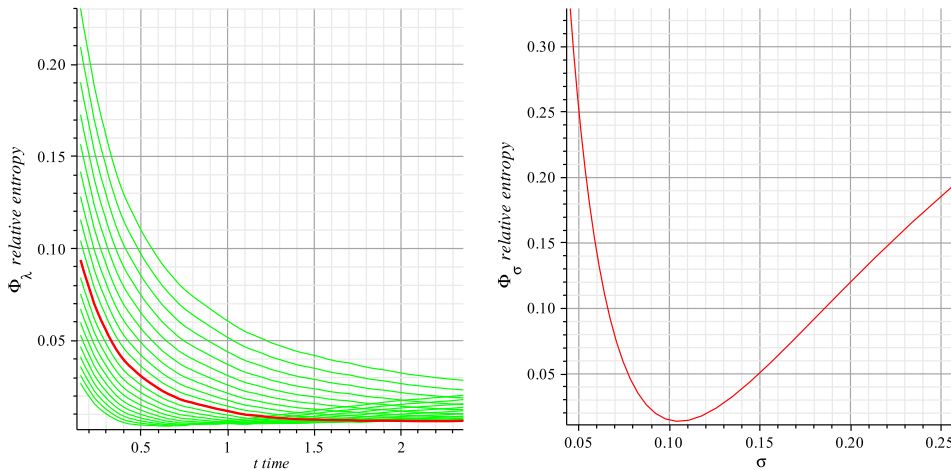


FIGURE 4. In these plots, the GBCD  $\rho$  is averaged over 5 trials. (left) The relative entropy of the grain growth simulation with energy density (5.1) for a sequence of  $\Phi_\lambda$  vs.  $t$  with the optimal choice  $\sigma \approx 0.1$  noted in red. (right) Relative entropy for an indicated range of values of temperature parameter  $\lambda$  at the terminal time  $t = 2.3$ . The minimum value of the relative entropy is  $\approx 0.01$ .

## 6. SUMMARY

Engineering the microstructure of a material is a central task of materials science and its study gives rise to a broad range of basic science issues, as has been long recognized. Central to these



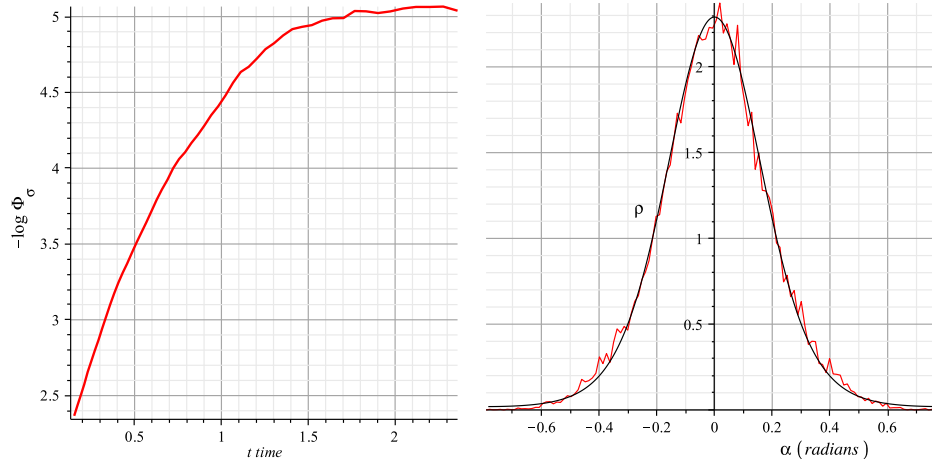


FIGURE 5. In these plots, the GBCD is averaged over 5 trials. (left) Plot of  $-\log \Phi_\sigma$  vs.  $t$  with energy density (5.1). It is approximately linear until it becomes constant showing that  $\Phi_\sigma$  decays exponentially. (right) GBCD  $\rho$  (red) and Boltzmann distribution  $\rho_\sigma$  (black) for the potential  $\psi$  of (5.1) with parameter  $\sigma \approx 0.1$  as predicted by our theory.

issues is the coarsening of the cellular structure. Here we have outlined an entropy based theory of the GBCD which is an upscaling of cell growth according to the two most basic properties of a coarsening network: a local evolution law and space filling constraints. The theory acomodates the irreversibility conferred by the critical events or topological rearrangements which arise during coarsening. It adds to the body of evidence that the evolution of the boundary network is the primary origin of texture development. It accounts both for the GBCD statistic and its kinetics by associating them with the mass transport implicit scheme. To our knowledge, this is the first implementation of the mass transport implicit scheme to the kinetic behavior of experimental systems. An undetermined temperature-like parameter is found by a convex dual problem reminiscent of a large deviation principle.

## ACKNOWLEDGEMENTS

Much of this research was done while E. Eggeling, Y. Epshteyn and R. Sharp were postdoctoral associates at the Center for Nonlinear Analysis at Carnegie Mellon University. We are grateful to our colleagues G. Rohrer, A. D. Rollett, R. Schwab, and R. Suter for their collaboration. Research supported by NSF DMR 0520425, DMS 0405343, DMS 0305794, DMS 0806703, DMS 0635983, DMS 0915013, DMS 1056821, DMS 1216433, OISE 0967140, DMS 1112984.

## References

- [1] B.L. Adams, D. Kinderlehrer, I. Livshits, D. Mason, W.W. Mullins, G.S. Rohrer, A.D. Rollett, D. Saylor, S Ta'asan, and C. Wu. Extracting grain boundary energy from triple junction measurement. *Interface Science*, 7:321–338, 1999.
- [2] BL Adams, D Kinderlehrer, WW Mullins, AD Rollett, and S Ta'asan. Extracting the relative grain boundary free energy and mobility functions from the geometry of microstructures. *Scripta Materiala*, 38(4):531–536, Jan 13 1998.
- [3] P. Bardsley. thesis, university of utah.
- [4] K. Barmak, E. Eggeling, M. Emelianenko, Y. Epshteyn, D. Kinderlehrer, R.Sharp, and S.Ta'asan. Predictive theory for the grain boundary character distribution. In *Materials Science Forum*, volume 715-716, pages 279–285. Trans Tech Publications, 2012.
- [5] K. Barmak, E. Eggeling, M. Emelianenko, Y. Epshteyn, D. Kinderlehrer, R. Sharp, and S. Ta'asan. Critical events, entropy, and the grain boundary character distribution. *Phys. Rev. B*, 83(13):134117, Apr 2011.
- [6] K. Barmak, E. Eggeling, M. Emelianenko, Y. Epshteyn, D. Kinderlehrer, and S. Ta'asan. Geometric growth and character development in large metastable systems. *Rendiconti di Matematica, Serie VII*, 29:65–81, 2009.

- [7] K. Barmak, E. Eggeling, D. Kinderlehrer, R. Sharp, S. Ta'asan, A.D. Rollett, and K.R. Coffey. Grain growth and the puzzle of its stagnation in thin films: The curious tale of a tail and an ear. *Progress in Materials Science*, 58(7):987 – 1055, 2013.
- [8] K. Barmak, M. Emelianenko, D. Golovaty, D. Kinderlehrer, and S. Ta'asan. On a statistical theory of critical events in microstructural evolution. In *Proceedings CMDS 11*, pages 185–194. ENSMP Press, 2007.
- [9] K. Barmak, M. Emelianenko, D. Golovaty, D. Kinderlehrer, and S. Ta'asan. Towards a statistical theory of texture evolution in polycrystals. *SIAM Journal Sci. Comp.*, 30(6):3150–3169, 2007.
- [10] K. Barmak, M. Emelianenko, D. Golovaty, D. Kinderlehrer, and S. Ta'asan. A new perspective on texture evolution. *International Journal on Numerical Analysis and Modeling*, 5(Sp. Iss. SI):93–108, 2008.
- [11] Katayun Barmak, Eva Eggeling, Maria Emelianenko, Yekaterina Epshteyn, David Kinderlehrer, Richard Sharp, and Shlomo Ta'asan. An entropy based theory of the grain boundary character distribution. *Discrete Contin. Dyn. Syst.*, 30(2):427–454, 2011.
- [12] Katayun Barmak, Eva Eggeling, Maria Emelianenko, Yekaterina Epshteyn, David Kinderlehrer, Richard Sharp, and Shlomo Ta'asan. A theory and challenges for coarsening in microstructure. In *Analysis and numerics of partial differential equations*, volume 4 of *Springer INdAM Ser.*, pages 193–220. Springer, Milan, 2013.
- [13] Jean-David Benamou and Yann Brenier. A computational fluid mechanics solution to the Monge-Kantorovich mass transfer problem. *Numer. Math.*, 84(3):375–393, 2000.
- [14] Lia Bronsard and Fernando Reitich. On three-phase boundary motion and the singular limit of a vector-valued Ginzburg-Landau equation. *Arch. Rational Mech. Anal.*, 124(4):355–379, 1993.
- [15] J.E. Burke and D. Turnbull. Recrystallization and grain growth. *Progress in Metal Physics*, 3(C):220–244, IN11–IN12, 245–266, IN13–IN14, 267–274, IN15, 275–292, 1952. cited By (since 1996) 68.
- [16] Robert Gomer and Cyril Stanley Smith, editors. *Structure and Properties of Solid Surfaces*, Chicago, 1952. The University of Chicago Press. Proceedings of a conference arranged by the National Research Council and held in September, 1952, in Lake Geneva, Wisconsin, USA.
- [17] M. Gurtin. *Thermomechanics of evolving phase boundaries in the plane*. Oxford, 1993.
- [18] C. Herring. Surface tension as a motivation for sintering. In Walter E. Kingston, editor, *The Physics of Powder Metallurgy*, pages 143–179. McGraw-Hill, New York, 1951.
- [19] C. Herring. The use of classical macroscopic concepts in surface energy problems. In Gomer and Smith [16], pages 5–81. Proceedings of a conference arranged by the National Research Council and held in September, 1952, in Lake Geneva, Wisconsin, USA.
- [20] Richard Jordan, David Kinderlehrer, and Felix Otto. The variational formulation of the Fokker-Planck equation. *SIAM J. Math. Anal.*, 29(1):1–17, 1998.
- [21] D Kinderlehrer, J Lee, I Livshits, A Rollett, and S Ta'asan. Mesoscale simulation of grain growth. *Recrystallization and grain growth, pts 1 and 2*, 467-470(Part 1-2):1057–1062, 2004.
- [22] D Kinderlehrer and C Liu. Evolution of grain boundaries. *Mathematical Models and Methods in Applied Sciences*, 11(4):713–729, Jun 2001.
- [23] D Kinderlehrer, I Livshits, GS Rohrer, S Ta'asan, and P Yu. Mesoscale simulation of the evolution of the grain boundary character distribution. *Recrystallization and grain growth, pts 1 and 2*, 467-470(Part 1-2):1063–1068, 2004.
- [24] David Kinderlehrer, Irene Livshits, and Shlomo Ta'asan. A variational approach to modeling and simulation of grain growth. *SIAM J. Sci. Comp.*, 28(5):1694–1715, 2006.
- [25] David Kinderlehrer and Xin Yang Lu. to appear.
- [26] Robert V. Kohn. Irreversibility and the statistics of grain boundaries. *Physics*, 4:33, Apr 2011.
- [27] W.W. Mullins. 2-Dimensional motion of idealized grain growth. *Journal Applied Physics*, 27(8):900–904, 1956.
- [28] W.W. Mullins. *Solid Surface Morphologies Governed by Capillarity*, pages 17–66. American Society for Metals, Metals Park, Ohio, 1963.
- [29] GS Rohrer. Influence of interface anisotropy on grain growth and coarsening. *Annual Review of Materials Research*, 35:99–126, 2005.
- [30] Anthony D. Rollett, S.-B. Lee, R. Campman, and G. S. Rohrer. Three-dimensional characterization of microstructure by electron back-scatter diffraction. *Annual Review of Materials Research*, 37:627–658, 2007.
- [31] Cyril Stanley Smith. Grain shapes and other metallurgical applications of topology. In Gomer and Smith [16], pages 65–108. Proceedings of a conference arranged by the National Research Council and held in September, 1952, in Lake Geneva, Wisconsin, USA.
- [32] John von Neumann. Discussion remark concerning paper of C. S. Smith "grain shapes and other metallurgical applications of topology". In Gomer and Smith [16], pages 108–110. Proceedings of a conference arranged by the National Research Council and held in September, 1952, in Lake Geneva, Wisconsin, USA.

K.B.: DEPARTMENT OF APPLIED PHYSICS AND APPLIED MATHEMATICS, COLUMBIA UNIVERSITY, NEW YORK, NY 10027

E.E.: FRAUNHOFER AUSTRIA RESEARCH GMBH, VISUAL COMPUTING, A-8010 GRAZ, AUSTRIA

M.E.: DEPARTMENT OF MATHEMATICAL SCIENCES, GEORGE MASON UNIVERSITY, FAIRFAX, VA 22030

Y.E.: DEPARTMENT OF MATHEMATICS, THE UNIVERSITY OF UTAH, SALT LAKE CITY, UT, 84112

D.K.: DEPARTMENT OF MATHEMATICAL SCIENCES, CARNEGIE MELLON UNIVERSITY, PITTSBURGH, PA 15213

R.S.: GLOBYS CORPORATION, SEATTLE, WA, 98104

S.T.: DEPARTMENT OF MATHEMATICAL SCIENCES, CARNEGIE MELLON UNIVERSITY, PITTSBURGH, PA 15213

*E-mail address:* kb2612@columbia.edu

*E-mail address:* eva.eggeling@fraunhofer.at

*E-mail address:* memelian@gmu.edu

*E-mail address:* epshteyn@math.utah.edu

*E-mail address:* davidk@cmu.edu

*E-mail address:* rsharp@gmail.com

*E-mail address:* shlomo@andrew.cmu.edu